Table 1: Parameter values

Discretization parameters		SDE
Discretization step	Δx	10^{-2}
Number of discretization steps	n_x	340
Time step	Δt	10^{-2}
Number of timesteps	n	10^6

-

1 Model problem

Until now, we considered a system of non-interacting particles. We will now extend our model to a mean field model by introducing a third parameter α, which is the degree of interaction or cooperation in the system. A simple form of cooperative behaviour is the case where each agent tends to follow the state of the majority (or, each particle feels an attractive force towards the mean state of the system). To include this cooperation effect in our stochastic simulation, we add this mean reversion term to the SDE (**??**):

$$\mathrm{d}x = \mu V(x)\mathrm{d}t + \sigma \mathrm{d}W_t + \alpha(\bar{x} - x)\mathrm{d}t, \tag{1}$$

with $\bar{x}(t) = \frac{1}{N}\sum_{i=1}^{N} x_i(t)$ denoting the empirical mean.

An interesting application of this model to banks and insurance is the emergence of systemic risk. Banks will try to minimize their own individual risk by spreading the risk between each other. However, this may increase the risk that they may all fail: reducing individual risk on a micro-scale can increase systemic risk on a macro-scale. Garnier, Papanicolaou and Yang already made use of the dynamics in eq. (1) to show that interconnectedness between agents indeed affects the stability of the whole system, causing systemic risk [**?**]. They defined x_i as the state of risk of agent i. The bi-stable-state structure of the potential $V(x)$ ensures that each risk variable stays around -1 (defined as the normal state) or $+1$ (the failed state). A natural measure of systemic risk is then the transition probability of the empirical mean $\bar{x}$ from the normal state to the failed state.

To establish the idea, let us repeat the numerical simulations with eq. 1. The evolution of the system is now characterized by by the initial conditions, the three parameters (μ, σ, α) and by the system size N. Figure 1 illustrates the behaviour of the empirical mean $\bar{x}$. The simulations were performed with all agents initially in the normal state. Nevertheless, if randomness dominates the interaction, the agents can move immediately to the other potential well. The system then behaves like N independent diffusions, and hence, by the symmetry of the potential, the mean state will be attracted to a single mixed state $\bar{x} = 0$. Upon increasing the interaction parameter α, however, we find two new macroscopic states, suggesting the precence of a pitchfork bifurcation at the macroscopic level. These solutions are no stable steady states, but rather coarse metastable states. Their lifetime is linked to the finite system size.

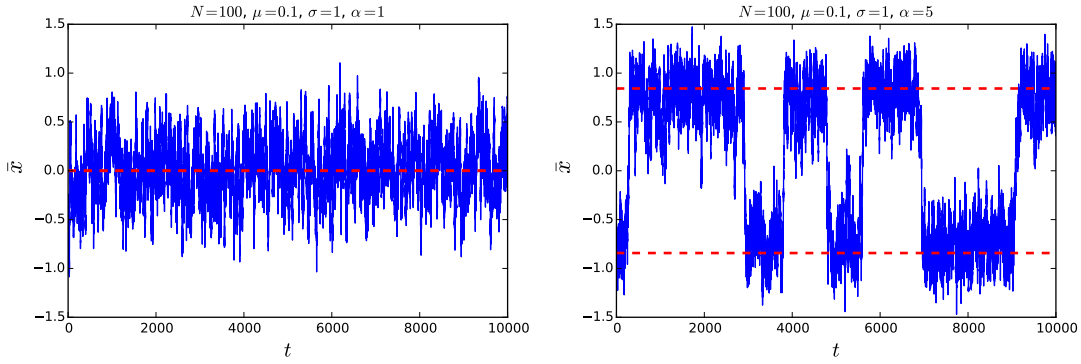

Figure 1: The empirical mean, simulated for different α. *Left*: the system has one single state $\bar{x} = 0$. *Right*: for $\alpha > \alpha_c$ two metastable equilibria emerge. The red dashed lines are approximated analytical solutions for the steady states.

1.0.1 Calculating fixed points

The steady states are computed with the Newton-Krylov solver described in section **??** and compared with the approximated analytical solutions, calculated by Garnier et. al for small h [**?**].

1.0.2 Continuation

We use a pseudo-arclength contunaution method with secant prediction steps. In fig. **??** we show a bifurcation diagram of the densities.

By adding the mean reversion term, the Fokker-Planck equation (**??**) describing the evolution of the density, now becomes

$$\frac{\partial \rho(x,t)}{\partial t} = -\mu \frac{\partial (f(x)\rho(x,t))}{\partial x} - \alpha \frac{\partial}{\partial x}\left[\left(\int x\rho(x,t)\mathrm{d}x - x\right)\rho(x,t)\right] + \frac{\sigma^2}{2}\frac{\partial^2 \rho(x,t)}{\partial x^2}. \quad (2)$$

Explicit solutions of eq. are not available in general, but we can find equilibrium solutions. Assuming that $\xi = \lim_{t\to\infty} \int x\rho(x,t)\mathrm{d}x$, an equilibrium solution satisfies

$$\mu \frac{\partial (f(x)\rho_\xi)}{\partial x} - \alpha \frac{\partial}{\partial x}\left[(\xi - x)\rho_\xi\right] + \frac{\sigma^2}{2}\frac{\partial^2 \rho_\xi}{\partial x^2} \quad (3)$$

-

In addition, the non-zero solutions $\pm\xi$ are

$$\xi = \pm\sqrt{1 - 3\frac{\sigma^2}{2\theta}}\left(1 + \ \mu\frac{6}{\sigma^2}(\frac{\sigma^2}{2\theta})^2\frac{1 - 2\frac{\sigma^2}{2\theta}}{1 - 3\frac{\sigma^2}{2\theta}}\right) + \mathcal{O}(\mu^2) \quad (4)$$

]

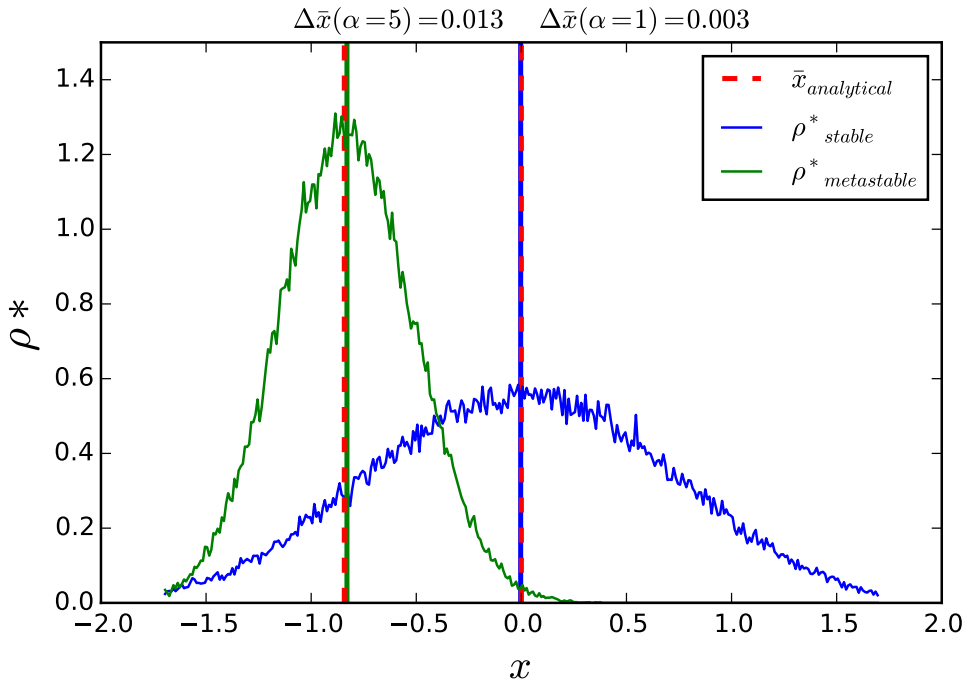

Figure 2

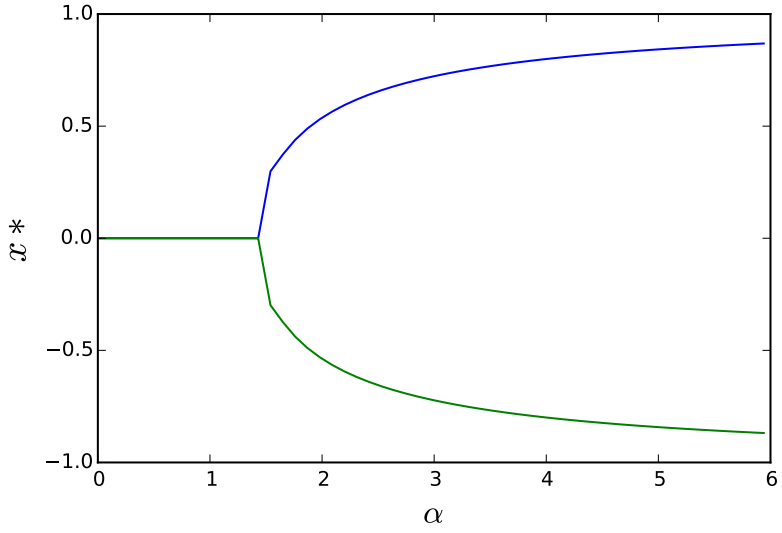

Figure 3

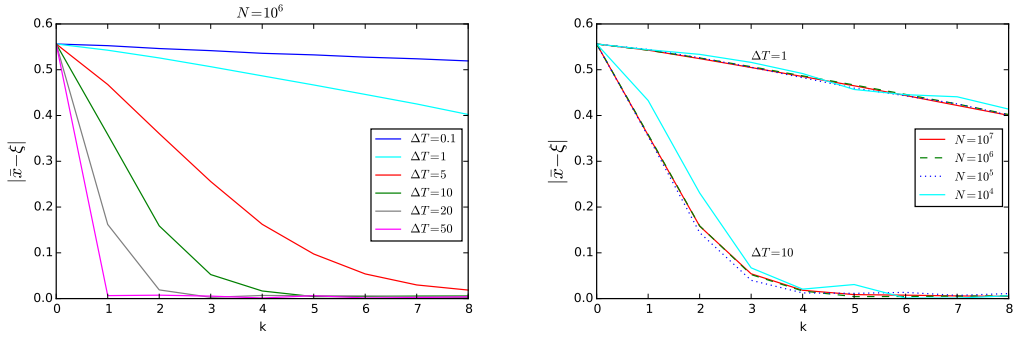

Figure 4: The bias between the analytical solution ξ and the mean $\bar{x}$ of the density calculated with the Newton-Krylov solver is plotted as a function of the number of Newton iterations k. This bias converges to zero with a rate depending on the timestep used in the coarse time stepper ΔT, but not on the number of particles N. ($\Delta x = 10^{-2}$, $\Delta t = 10^{-2}$, $\mu = 0.05$, $\alpha = 5$, $\sigma = 1$)

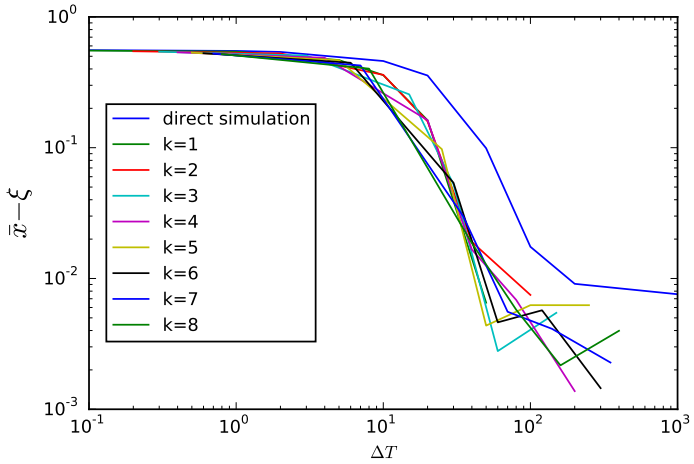

Figure 5: The total number of timesteps used in the Newton-Krylov-method is lower than the number of timesteps in direct simulation to calculate a fixed point with the same accuracy. ($N = 10^6$,$\Delta x = 10^{-2}$, $\Delta t = 10^{-2}$, $\mu = 0.05$, $\alpha = 5$, $\sigma = 1$)

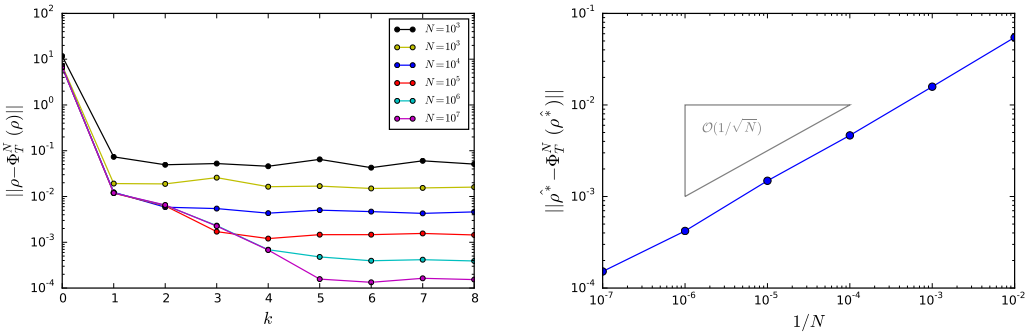

Figure 6: The needed number of Newton iterations and the tolerance after convergence depend on the number of particles N (*left*). This best achieved tolerance converges to zero with $\mathcal{O}(\frac{1}{\sqrt{N}})$ (*right*). (Parameter values: $\Delta x = 10^{-2}$, $\Delta t = 10^{-2}$, $\Delta T = 10$ $\mu = 0.05$, $\alpha = 5$, $\sigma = 1$, $\epsilon_{\texttt{GMRES}} = 10^{-5}$)